Macromolecules

ARTICLE

pubs.acs.org/Macromolecules

Nanoscale Phase Separation of P3HT PCBM Thick Films As Measured by Small-Angle X-ray Scattering

Andrew J. Parnell,*[,†] Ashley J. Cadby,[†] Oleksandr O. Mykhaylyk,[‡] Alan D. F. Dunbar,[∥] Paul E. Hopkinson,[⊥] Athene M. Donald,[⊥] and Richard A. L. Jones[†]

[†]Department of Physics and Astronomy, The University of Sheffield, S3 7RH, United Kingdom

[‡]Department of Chemistry, The University of Sheffield, S3 7HF, United Kingdom

[∥]Department of Chemical and Biological Engineering, The University of Sheffield, United Kingdom

[⊥]Department of Physics, Cavendish Laboratory, University of Cambridge, JJ Thomson Avenue, Cambridge CB3 0HE, United Kingdom

Supporting Information

ABSTRACT: The elusive and difficult to measure phase separation length scale in poly(3-hexylthiophene):C61-butyric acid methyl ester (P3HT:PCBM) bulk heterojunction layers was measured using small-angle X-ray scattering (SAXS) from thick films of the blend. After drop-casting and allowing the material to dry, there was a distinct nanoscale phase separation of the two blend components as measured by SAXS. Thermal annealing reduced the degree of phase separation as qualitatively measured by the decrease in the SAXS invariant, and the phase separation length scale was virtually unchanged at 25 nm. We attribute this reduction in the SAXS invariant to diffusion of PCBM into the amorphous P3HT; this was also confirmed by a reduction in the photoluminescence (PL) and a small reduction in the PL lifetime. We show that a bulk heterojunction system blend of 1:0.7 P3HT:PCBM is not just a simple two-phase system with well-defined interfaces, but instead it is a much more complicated system incorporating regions of crystalline P3HT, PCBM, and a mixed phase of amorphous P3HT and PCBM. Our work confirms that PCBM penetrates into P3HT upon thermal annealing and so reinforces the view proposed by Kiel et al. [Phys. Rev. Lett. 2010, 105, 168701]. We suggest that, alongside device testing this type of thick film, SAXS experiments would aid efficiency improvements by permitting measurement of the phase separation length scale in bulk heterojunction organic photovoltaic materials. This is a key parameter for understanding and designing improved polymer solar cells.

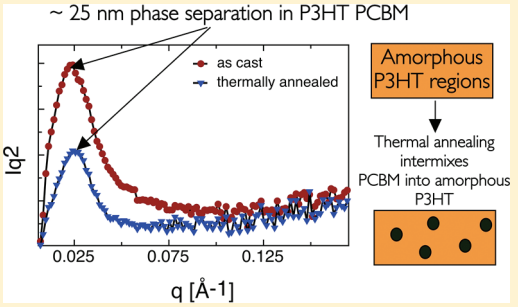

INTRODUCTION

So far, a number of studies have examined the degree of phase separation in P3HT PCBM blends using techniques including atomic force microscopy (AFM), transmission electron microscopy (TEM), and grazing incidence X-ray scattering (GISAXS). Chiu et al. used GISAXS to probe device comparable systems and concluded that after thermal annealing the PCBM had domain sizes of greater than 20 nm and P3HT crystallites larger than 16 nm.[1] It is difficult and uncommon to scale GISAXS data as well as to perform the necessary background corrections that are standard practice in conventional transmission SAXS. This makes it hard to compare the same illuminated volume between samples due to small changes in angle and volume of the sample upon thermal annealing. AFM and GISAXS are highly surface sensitive techniques.

TEM allows the whole depth of the sample to be imaged, but the similarities in mass−thickness between components results in extremely weak material contrast. Enhancement of any inherent contrast present can be achieved by defocusing the microscope objective lens, thus altering the modulation-transfer function and enhancing the contrast at length scales commensurate with the phase separation distance.[2] However, when performing defocused electron microscopy, it is important to bear in mind that defocus also leads to spatial filtering by the microscope, arising from the form of the contrast transfer function.[3] Thus, as was established for atactic polymers such as polystyrene more than 30 years ago, "salt and pepper" structures with a well-defined periodicity can be observed by defocused TEM, even when there is no intrinsic structure present (see the paper by Uhlmann[4] and subsequent comment by Thomas[5] for a detailed discussion of these points). Much more thorough investigations than a single image at some defocus, including a detailed through-focus series, need to be carried out to confirm the presence of real phase separation when using this approach. Additionally, any actual structures present may superpose through the thickness of the film, further complicating image interpretation, unless the film thickness is commensurate or less than the length scale of any putative structure present.

Received: April 2, 2011
Revised: June 22, 2011
Published: July 21, 2011

 © 2011 American Chemical Society

These complexities throw into question the results obtained by Moon et al.,[6] who applied this method to a cross ection of a device prepared by focused ion-beam (FIB) milling, determining a length scale of 25 nm for an annealed 1:0.7 P3HT:PCBM blend film. As this method is extremely sensitive to the change in defocus, there are a number of checks and balances that need to be performed to prevent ambiguities in the resulting analysis of the data. Recent work[7] comparing images seen in amorphous pure polystyrene film with a cross section of a P3HT:PCBM blend reinforces the earlier message about structures being visible in polystyrene and the difficulties in interpreting these types of images as proof of any intrinsic phase separation.

On the other hand, electron tomography does not require defocus and benefits from improved signal-to-noise ratio but is only sensitive to the crystalline P3HT component of the blend.[8] This type of measurement has shown P3HT nanowires with a diameter of 15 nm. Differences in the P3HT and PCBM plasmon peak energies allow structures to be observed by energy filtered TEM (EFTEM); these measurements also show P3HT nanowires, with a diameter of ~10 nm and a structural length scale of 25 nm.[9]

GISAXS measurements using resonant soft X-ray scattering have detected a length scale of ~20 nm for the phase separation of an annealed 150 nm thick P3HT:PCBM blend film.[10] Another study by Veploegen et al. used GISAXS and measured a value of 16 nm.[11] Understanding the dynamics of phase separation and using this knowledge to inform device optimization will help to give an empirical understanding of polymer solar cell structure and efficiency. The phase separation length scale is crucially important, as it dominates the efficiency of an organic photovoltaic device (OPV) by controlling the exciton separation efficiency. When a photon of light interacts with an OPV material, first it must be absorbed, after which time a short-lived excited state known as an exciton is generated; this is a weakly bound state of a hole and an electron and must be dissociated into separate charges for OPV operation. The conventional wisdom is that charge separation takes place at the interface of the two blend materials. An exciton has a short lifetime of the order of ~nanoseconds (corresponding to a diffusion distance of ~10 nm),[12] before which it must be split into an electron and a hole; otherwise, it will relax to the ground state and as such is wasted.

We have used small-angle X-ray scattering (SAXS) to quantify the phase separation length scale in device applicable blends of conjugated P3HT:PCBM systems for organic photovoltaics. The SAXS technique probes differences in electron density, ρ, and as there is a large electron density contrast difference between the pure blend materials, P3HT and PCBM (ρ_{P3HT} = 0.358 electrons/Å^3 and ρ_{PCBM} = 0.458 electrons/Å^3, respectively), it is ideally suited to study the phase separation in these polymer blend systems. It is also a bulk measurement; the technique samples a relatively large volume (the cross section of the beam is usually a few hundreds of square micrometers), thus giving a global picture of the sample which overcomes the limited sampling statistics associated with TEM. In order to measure a P3HT:PCBM blend using SAXS, it was necessary to look at thick films (films of the order of several micrometers) as the amount of scattered intensity was too low using an actual OPV device layer thickness of ~150 nm.

Although the samples studied are much thicker than actual device samples, our processing results in samples which demonstrate effects similar to those observed for slowly dried films by Li et al. where they studied the effect of drying kinetics on the resultant P3HT:PCBM blend, which had profound effects on the final device characteristics.[13] They found that films dried slowly had better performance characteristics (higher external quantum efficiency, higher power conversion efficiency, higher fill factor, and lower series resistance) than the rapidly dried films. Their work also studied the charge carrier mobility of holes and electrons using time-of-flight measurements for 1 μm thick blend films and saw more balanced transport as well as nondispersive transport for the slowly dried film, whereas the rapidly dried film displayed dispersive dynamics and unbalanced transport. All these differences in performance can be explained by the rate of solvent evaporation, as fast solvent loss quenches the phase separation process, and consequently the longer the blend is mobile and contains solvent the more the mixture will proceed to a more phase separated state. The driving force for phase separation in polymer blends during spin-coating is based on the thermodynamic theories of polymer mixing and differences in the solubility parameters of the two polymers in a common solvent.[14,15] In our work we aimed to study a well-phase-separated system and so allowed the samples to dry slowly.

EXPERIMENTAL SECTION

Materials and Film Preparation. P3HT was obtained from Merck (UK) (Batch SP0001 94.2% regioregularity with specified M_w = 54 200 Da and M_n = 23 600 Da). The PCBM was obtained from Solenne BV. Solutions of P3HT and PCBM were prepared separately in filtered (0.45 μm PALL Corp.) chlorobenzene at a concentration of 50 mg/mL. The two solutions were then mixed in a proportion of 1:0.7 (P3HT:PCBM) by volume. Prior to drop-casting, the blend solution was heated to 75 °C to molecularly dissolve all the material. The solutions were drop-cast onto clear ruby-grade mica discs, 25 μm thick and 15 mm diameter (Attwater group, UK); the drop-cast films took ~20 min to dry. The film drying was monitored using a laboratory digital balance (Sartorius AE160). Solvent loss for a drop-cast film throughout the drying stage was measured to determine the point at which drying stops (the layers become dry). This data are presented in Supporting Information Figure SI 1.

Two sample sets were made; one set drop casting immediately after heating and another set where the solution had been left for 7 days after heating (the SAXS data for this set showed a similar phase separation length scale and are in the Supporting Information Figure SI 2). The annealed samples were heated using a hot stage (Linkam Scientific Instruments Ltd., Tadworth, UK) at 150 °C for an hour in air.

X-ray Measurements. The SAXS experiments were carried out using a laboratory-based BrukerAXS Nanostar (Cu Kα radiation, wavelength λ = 1.54 Å, 2D HiStar multiwire detector) equipped with a semitransparent beamstop for normalization of the scattering patterns. The SAXS camera length was set to 1.05 m, which allowed patterns corresponding to scattering vectors 0.01 Å^{-1} < q < 0.2 Å^{-1} ($q = (4\pi \sin\theta)/\lambda$, where 2θ is the scattering angle) to be recorded. WAXS measurements were carried out using the same instrument set to the shortest camera mode (0.2 Å^{-1} < q < 1.7 Å^{-1}). The patterns recorded by the Nanostar were subjected to flat field and spatial corrections, incident beam intensity normalization, and a background subtraction. The normalization of the WAXS and SAXS data was performed using intensity of the direct X-ray beam passed through the sample recorded after the semitransparent beam stop located in front of the detector; this allows true scaling of the data to flux and thickness. A STOE STADI P X-ray diffractometer (Cu Kα_1 radiation) was also used to record diffraction patterns for the diffraction peak broadening analysis. Diffraction peaks of P3HT have been corrected for instrumental broadening using the Stokes method (Fourier deconvolution)[16] to measure their physical broadening [calculated as integral breadth $\beta_f^{hkl} = \int I_f^{hkl}(2\theta)$

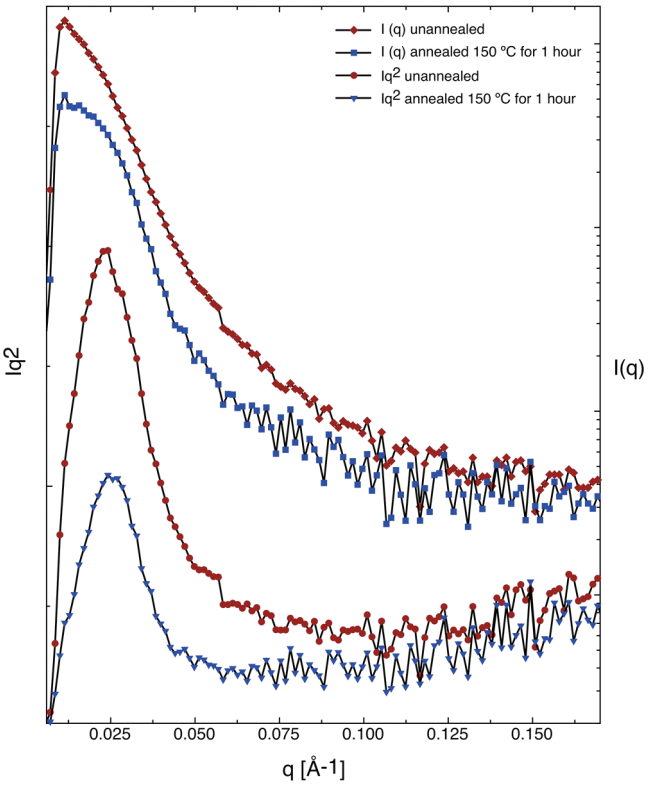

Figure 1. SAXS data for thick drop-cast films of P3HT:PCBM on thin mica substrates. The data are plotted in two forms: scattering intensity $I(q)$ versus scattering vector q (axis on the right in logarithmic scale) and Iq^2 versus q (axis on the left) representing the Lorentz-corrected data.

$d(2\theta)/I_f^{hkl}(2\theta_{hkl})$, where $I_f^{hkl}(2\theta)$ is the deconvoluted pattern of the diffraction peak, $2\theta_{hkl}$ is the peak position, and *hkl* denotes the Miller indices of the peak] related to the crystallite size via the Scherrer equation [$D = \lambda/(\beta_f^{hkl} \cos \theta_{hkl})$, where θ_{hkl} is half the diffraction angle of the analyzed peak and β_f^{hkl} is in radians]. Both silicon standard and mica reflections, observed in the diffraction patterns from the sample substrate, have been used to estimate the instrumental broadening of the diffractometer. It was found that the instrumental broadening was an order of magnitude less than the width of the diffraction peaks studied.

Optical Characterization. Optical absorption measurements were performed using a 60 W tungsten lamp as a light source. Light from the lamp was focused through the blades of a Stanford Research Systems optical chopper, through the sample under investigation and onto the slits of a SPEX 1/3 m monochromator and detected with a silicon diode using a lock-in amplifier. The transmission spectra of the samples and a blank mica reference sample were recorded, and the optical densities (OD) of the samples were calculated using Beer's law. Although the samples were optically dense, the signal recorded by the lock-in amplifier was always greater than the background noise level throughout the measurement.

For photoluminescence (PL) measurements the samples were illuminated with 532 nm monochromatic light from a Spectra-Physics Mira laser. PL spectra were collected in reflection geometry and recorded using an Andor Shamrock spectrometer with a cooled CCD. The optical density of the samples was high enough that collection in a reflecting geometry allowed for a comparison in PL intensity between samples. As due to the thickness of the sample, we assume that very few of the photons are transmitted through the entire thickness of the film, enabling us to compare the quantum yields. Photoluminescence lifetimes were measured by exciting the samples with 430 nm monochromatic light from a frequency-doubled Spectra Physics TI sapphire laser, the PL signal was collected using a PicoQuant avalanche photodiode, and a 40 nm band-pass filter centered at 700 nm was used to isolate the PL. Time-correlated single photon counting was performed using a Becker and Hickle 830 TCSPC card.

RESULTS AND DISCUSSION

In Figure 1, a subtle hump can be identified in the $I(q)$ SAXS data at a $q \sim 0.025$ Å^{-1}. The position of the hump corresponds to the phase separation length scale seen between the two blend components.[17] We have also plotted the SAXS data as an Iq^2 versus q plot, known as the Lorentz-corrected scattered intensity, representing the data with no aberrations originating from the scattering experiment geometry, enabling the position of the SAXS peak to be observed and measured.[17]

The integral of Iq^2 is called the invariant Q (as given in eq 1) and is a measure of the degree of phase separation in the system; it is independent of size or structural morphology and is linearly related to the electron density variance $\langle \eta^2 \rangle$ within the system.[18]

$$Q = \int_0^\infty I(q) q^2 \, dq \propto \langle \bar{\eta}^2 \rangle \tag{1}$$

For a two-phase sytem $\langle \bar{\eta}^2 \rangle = \phi_1 \phi_2 (\rho_1 - \rho_2)^2$, where ϕ_1 and ϕ_2 are fractions of the components and ρ_1 and ρ_2 are electron densities of the components.

For the as-cast sample we can see that the degree of phase separation is greater than after the samples have been annealed at 150 °C for an hour, and so annealing reduces the SAXS invariant. The 2D SAXS patterns were presented by an isotropic ring, suggesting that the as-cast film has phase-separated nanostructure of P3HT and PCBM with no preferred orientation. The as-cast sample and the thermally annealed sample have a peak corresponding to length scale 26.5 and 25.1 nm, respectively (see Supporting Information Table 1 for q values). The phase separation length scale measured using SAXS is very similar to that measured by EFTEM (25 nm).[9] Our data show that the bulk length scale measured in these layers is then very similar to that in actual device thickness films. This correlation suggests that SAXS can be used to optimize OPV device performance by allowing a study of the parameters that influence the phase separation length scale. The effect of thermal annealing on spin-cast films had been presumed to cause an increase in the phase separation between the P3HT and PCBM alongside improvements in the ordering and an enhancement in the crystallinity of P3HT; this ordering has a big impact on the absorption spectra of P3HT:PCBM blend devices.[19−21]

To understand the reduction in the invariant upon annealing, we need to remember that any scattering is the product of differences in electron density. The maximum in the invariant would occur when there are pure domains of the two components. As they become more intermixed forming homogenized areas in the sample, there will be a reduction in the electron contrast and a concomitant decrease in the invariant. In this respect two possible assumptions can be made to account for the reduction in electron contrast: (1) crystallization of amorphous P3HT on annealing increases the amount of material in the film which has less electron density contrast in relation to PCBM; (2) intermixing of the two components (P3HT and PCBM). By applying Scherrer's relation, it is possible to calculate the crystallite size of the P3HT crystals from the two pronounced diffraction peaks in the WAXS data corresponding to the crystal phase (Figure 2).[22]

dx.doi.org/10.1021/ma2007706 |*Macromolecules* 2011, 44, 6503–6508

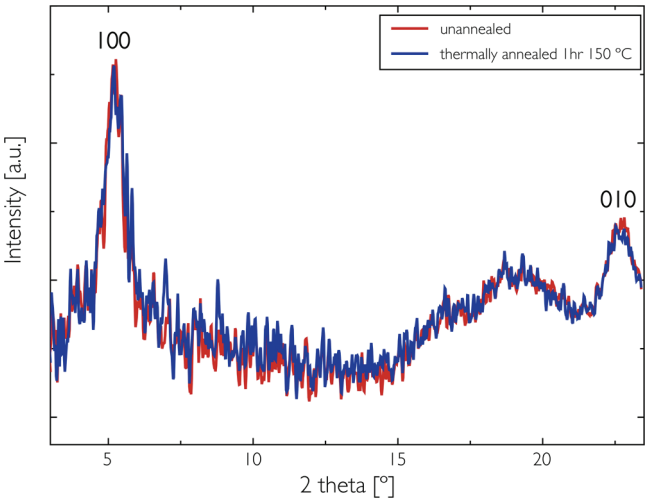

Figure 2. Normalized wide-angle X-ray scattering data of P3HT PCBM blend films showing the 100 and 010 peaks. The data were obtained using the Bruker Nanostar instrument and normalized using the semi-transparent beam stop.

The annealed sample as well as the as-cast sample produced a similar physical broadening for all analyzed peaks with $b_f \sim 1$ degree; however, peaks in the annealed sample are systematically narrower (see diffractometer data in Figure SI 4). The calculated P3HT crystallite size in the as-cast sample is $D = 8.3 \pm 0.6$ nm and in the annealed sample is $D = 9.6 \pm 0.5$ nm. Since both diffraction peaks corresponding to the same sample had a similar broadening, this suggested that strain in the P3HT crystal structure is negligible, and the observed broadening mainly originates from crystallite size. The slight growth in P3HT crystal size observed upon annealing is a reflection of the system reducing the total interfacial energy and moving to a lower energy state. The fact that the total amount of crystalline material has remained constant (the diffraction intensity of the normalized WAXS patterns does not change; see Figure 2), suggesting that the crystalline P3HT component remains virtually unaffected by the annealing process and that the observed decrease in the SAXS invariant intensity after annealing should be related to the intermixing of P3HT and PCBM during annealing and not due to an increase in the amount of crystalline material in the layer.

The phase-separated domains do not increase in size upon annealing according to our SAXS data. The phase separation length scale has actually reduced by ~5%. This could be due to some relaxation upon heating and removal of the residual drying stresses imposed as the layer dried from solution. To clarify, we saw no evidence of large PCBM aggregates on the surface of the film after thermal annealing either at the nanoscale using tapping mode AFM (Figure SI 5) or microscopically using optical microscopy (data not shown).

The absorption spectra in Figure 3, although differing in intensity due to changes in thickness, show very similar peak shapes, with the exception of a low-energy feature at 700 nm. Both spectra have a falloff in absorption at 650 nm consistent with crystalline P3HT.[23,24] We have tested our experimental setup on much thinner spin-coated P3HT films where we do see the commonly noted three peaks (522, 550, and 605 nm; see Supporting Information Figure SI 6). We attribute their absence in the thicker films to a broadening of the peaks and loss of resolution due to scattering effectively smearing out the peaks. The low-energy feature centered at 700 nm appears in the annealed sample but is absent from the as cast sample; we attribute this peak to $PC_{60}BM$, and it has been seen previously by others[25] in the absorption spectra of thick $PC_{60}BM$ and C_{60} films.[26] It has been assigned to a triplet transition and also tentatively explained due to distortion of the C_{60} shape.[26]

With such optically thick samples we can compare the reflected photoluminescence (PL) intensities between the two samples to give us an insight into any relative changes in the quantum efficiency of the samples due to annealing. The PL data show a reduction in intensity upon annealing becoming more quenched, an indication that the two components are in closer proximity after annealing. The photoluminescence lifetime of the two samples has been measured by excitation at 430 nm by a Ti:sapphire laser. The system response function was 65 ps. In previous studies a biexponential decay was used to fit decay curves in these systems. The biexponential decay can be associated with a two-step process with the shorter component of the fit being dominated by exciton splitting and the longer component due to exciton migration. Our time correlated single photon counting system (TCSPC) cannot resolve the short-lived decay as it is below the time resolution of the detector. However, the longer lived lifetime can be resolved; for the annealed sample it was 119 ps while the lifetime for the as cast sample was 123 ps. These two lifetimes are very similar, and as the lifetimes are associated with migration this would imply that exciton migration in both samples is similar. Both systems also show a very weak (less than 5% of the entire curve) long-lived emission at 800 ps for a drop-cast sample and 740 ps for an annealed sample. This is very similar to that found for pure P3HT films. Considering the difference in quantum yield between pure P3HT and a P3HT/PCBM blend and the relative weakness of this lifetime component (less than 5%), this emission from seemingly isolated polymer is minimal.

Thus, at this point only the second option for the reduction in electron contrast remains to be discussed as the optical properties of the as-cast and thermally annealed sample underpin our interpretation of the SAXS and X-ray diffraction data.

The invariant reduction is most likely to be due to diffusion of PCBM into the amorphous P3HT regions of the film upon thermal annealing.[27] There is a recent body of evidence demonstrating a mixed phase of P3HT and PCBM upon heating.[22,28,29] These studies have mostly been secondary ion mass spectroscopy studies looking on the tens of nanometers scale at intermixing, using bilayers of P3HT and PCBM and following the kinetics of mixing upon heating, which are rapid at temperatures near 150 °C. Recent work using near-edge X-ray absorption fine structure (NEXAFS) has shown that PCBM is soluble in regiorandom P3HT at up to 20 wt %, showing that pure phases of amorphous P3HT do not exist in P3HT:PCBM blends after annealing.[29]

Small-angle neutron scattering (SANS) studies on 1:1 P3HT:PCBM blend thin films by Kiel et al. examined the change in scattering and consequently the location of PCBM upon thermal annealing the film (at 140 °C for 20 min). They found that ~15 vol % PCBM is dissolved in the P3HT after thermal annealing. It was problematic to identify conclusively that the dissolved PCBM was located in the amorphous P3HT; however, they suggested this as the probable location.[30] Other SANS work by Chen et al. has shown phase separation and a bicontinuous morphology for thin P3HT:PCBM blends upon annealing with crystalline domains of P3HT ~ 10 nm in size, similar to the measured values obtained in our work. Their study also confirmed that the diffusion of PCBM is rapid (a few seconds) at 150 °C and suggested that the PCBM diffuses through the amorphous part of P3HT regions.[27]

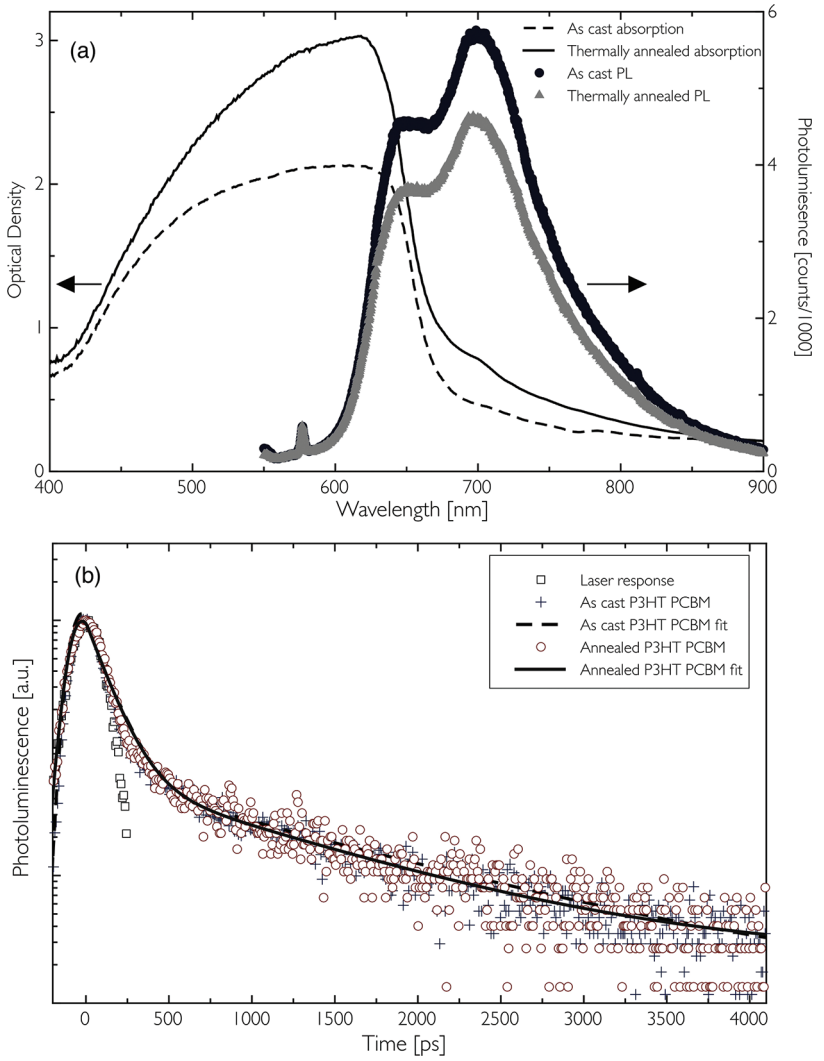

Figure 3. (a) Absorption and photoluminescence spectra for the thick samples before and after annealing. The photoluminescence (PL) spectra for the thick film samples, annealed and as-cast samples. The PL exhibits vibronic structure from the ordered crystalline P3HT. (b) PL lifetime data for the as-cast and thermally annealed sample as well as the response from the laser.

In our study it is possible to estimate the amount of PCBM diffused into P3HT upon annealing from the SAXS results (Figure 1) by making some assumptions: we are dealing with a two-phase system (PCBM, $\theta_1 = 0.41$; P3HT, $\theta_2 = 0.59$); the electron densities of both crystalline and amorphous P3HT are similar; the amount of crystalline P3HT does not change under annealing; PCBM diffuses into P3HT under annealing; the q range recorded in our SAXS experiments contains the majority of the scattered intensity. It can be found that the Q invariant is 1.76 times less after thermal annealing (Figure 1). In accordance with eq 1, such a decrease of the invariant should be associated with a diffusion of PCBM into P3HT, making a mixed phase of 13 vol % PCBM and 87 vol % P3HT. This estimation suggests that about 30% of the toal PCBM (0.13/0.41 × 100%) diffuses into P3HT. The obtained value is in agreement with the other studies on the incorporation of PCBM into amorphous P3HT by Kiel et al.[30] and Collins et al.[29]

■ CONCLUSIONS

In conclusion, we have measured the phase separation length scale to be ~25 nm both before and after thermal annealing using SAXS. We have also examined the change in the SAXS invariant and have seen that for a well-phase-separated sample, thermal annealing causes a reduction in the phase separation and a diffusion of PCBM into the amorphous P3HT. This conclusion is confirmed from the reduction in the intensity of the PL spectra upon annealing, implying a reduction in the distance between the two blend components. This work holds important implications for understanding the processing of organic solar cell blends as the conventional wisdom is that the P3HT:PCBM system is a simple two phase bulk heterojunction with well-defined interfaces between regions of approximately pure P3HT and pure PCBM; indeed, numerous cartoon depictions have helped to propagate this view.[31,32] Our results demonstrate that this assumption is not correct, but instead this is a more complicated system incorporating regions of crystalline P3HT, PCBM, and intermixed regions of amorphous P3HT and PCBM. Upon annealing there is diffusion of PCBM into the amorphous P3HT and comparatively little change in the crystallinity of P3HT and PCBM. We also found from WAXS measurements that the level of crystallinity before and after annealing remained constant, due in part to the slow drying of the samples, which is equivalent to solvent annealing.

dx.doi.org/10.1021/ma2007706 |*Macromolecules* 2011, 44, 6503–6508

The strongly intermixed region of PCBM and P3HT will increase the likelihood of an exciton being separated as the distance between PCBM and P3HT will be greatly reduced so understanding the impact of this mixed phase on device performance will make an important contribution to our understanding and improvement of organic photovoltaics. We have demonstrated that the SAXS technique is a very straightforward way of measuring the length scale and degree of phase separation in solar cell blend systems. These quantities, which are very difficult to measure with other techniques, can be correlated with the optical properties to obtain structure−property relations in solar cell materials, which are of paramount importance for improving the performance of organic solar cell devices. This technique is considerably easier in terms of both experimental settings and analysis when compared to the commonly employed GISAXS techniques.

■ ASSOCIATED CONTENT

Supporting Information. Further SAXS data for an alternate sample set, along with a table of the fitted peak positions and the extracted length scales along with the Scherrer data analysis; scaled WAXS data included for both sample sets as well as representative AFM scans for the as cast and thermally annealed case; a drying curve for a drop-cast sample, as a measure of the thick film layer drying time; optical absorption data for a spin-cast P3HT film measured using a commercial spectrometer and the optical equipment used to measure the thick blend films. This material is available free of charge via the Internet at http://pubs.acs.org.

■ AUTHOR INFORMATION

Corresponding Author
*E-mail: a.j.parnell@sheffield.ac.uk.

■ ACKNOWLEDGMENT

A.J.P. was funded by the EPSRC under grant EP/E046215/1 and P.E.H. via EPSRC grant EP/F019297/1. This works forms part of the UK Optimisation of Photovoltaics (UKOPV) collaboration. We thank Dr. Patrick Fairclough, Professor Tony Ryan and Andrew Pearson for helpful discussions and Dr. Nik Reeves-McLaren for acquiring the diffractometer data.

■ REFERENCES

(1) Chiu, M. Y.; Jeng, U. S.; Su, C. H.; Liang, K. S.; Wei, K. H. *Adv. Mater.* **2008**, *20* (13), 2573–2578.
(2) Williams, D. B.; Carter, C. B. *Transmission Electron Microscopy: A Textbook for Material Scientists*; Plenum Press: New York, 1996.
(3) Sawyer, L.; Grubb, D. T.; Meyers, G. F. *Polymer Microscopy*; Springer: Berlin, 2008.
(4) Uhlmann, D. R. *Faraday Discuss. Chem. Soc.* **1979**, *68*, 87–95.
(5) Thomas, E. L. *Faraday Discuss. Chem. Soc.* **1979**, *68*, 122–125.
(6) Moon, J. S.; Lee, J. K.; Cho, S.; Byun, J.; Heeger, A. J. *Nano Lett.* **2010**, *9* (1), 230–234.
(7) Kiel, J. W.; Kirby, B. J.; Majkrzak, C. F.; Maranville, B. B.; Mackay, M. E. *Soft Matter* **2010**, *6*, 641–646.
(8) van Bavel, S. S.; Sourty, E.; de With, G.; Loos, J. *Nano Lett.* **2009**, *9*, 507–513.
(9) Herzing, A. A.; Richter, L. J.; Anderson, I. M. *J. Phys. Chem. C* **2010**, *114*, 17501–17508.
(10) Swaraj, S.; Wang, C.; Yan, H.; Watts, B.; Lüning, J.; McNeill, C. R.; Ade, H. *Nano Lett.* **2010**, *10*, 2863–2869.
(11) Verploegen, E.; Miller, C. E.; Toney, M. F. *Synchrotron Radiat. News* **2010**, *23* (4), 16–21.
(12) Halls, J. J. M.; Pichler, K.; Friend, R. H.; Moratti, S. C.; Holmes, A. B. *Appl. Phys. Lett.* **1996**, *68*, 3120–3122.
(13) Li, G.; Shrotriya, V.; Huang, J.; Yao, Y.; Moriarty, T.; Emery, K.; Yang, Y. *Nature Mater.* **2005**, *4*, 864.
(14) Dunbar, A. D. F.; Mokarian-Tabari, P.; Parnell, A. J.; Martin, S. J.; Skoda, M. W. A.; Jones, R. A. L. *Eur. Phys. J. E* **2010**, *31* (4), 369–375.
(15) Heriot, S. Y.; Jones, R. A. L. *Nature Mater.* **2005**, *4*, 782.
(16) Stokes, A. R. *Proc. Phys. Soc.* **1948**, *61*, 382.
(17) Ophir, Z.; Wilkes, G. L. *J. Polym. Sci., Polym. Phys.* **1980**, *18*, 1469.
(18) Glatter, O.; Kratky, O. *Small Angle X-ray Scattering*; Academic Press: New York, 1982.
(19) Campoy-Quiles, M.; Ferenczi, T.; Agostinelli, T.; Etchegoin, P. G.; Kim, Y.; Anthopoulos, T. D.; Stavrinou, P. N.; Bradley, D. D. C.; Nelson, J. *Nature Mater.* **2008**, *7*, 158.
(20) Shin, M.; Kim, H.; Park, J.; Nam, S.; Heo, K.; Ree, M.; Ha, C.; Kim, Y. *Adv. Funct. Mater.* **2010**, *20*, 748–754.
(21) Kim, Y.; Cook, S.; Tuladhar, S. M.; Choulis, S. A.; J., N.; Durrant, J. R.; Bradley, D. D. C.; Giles, M.; McCulloch, I.; Ha, C.-S.; Ree, M. *Nature Mater.* **2006**, *5*, 197–203.
(22) Treat, N. D.; Brady, M. A.; Smith, G.; Toney, M. F.; Kramer, E. J.; Hawker, C. J.; Chabinyc, M. L. *Adv. Energy Mater.* **2011**, *1*, 82–89.
(23) Wang, T.; Dunbar, A. D. F.; Staniec, P. A.; Pearson, A. J.; Hopkinson, P. E.; Macdonald, J. E.; Lilliu, S.; Pizzey, C.; Terrill, N. J.; Donald, A. M.; Ryan, A. J.; Jones, R. A. L.; Lidzey, D. G. *Soft Matter* **2010**, *6*, 4128.
(24) Jannsen, G.; Aguirre, A.; Goovaerts, E.; Vanlaeke, P.; Poortmans, J.; Manca, J. *Eur. Phys. J. Appl. Phys.* **2007**, *37*, 287–290.
(25) Chen, E.-N.; Chang, C.-Y.; Shieh, J.-T.; Tseng, S.-R.; Meng, H.-F.; Hsu, C.-S.; Horng, S.-F. *Appl. Phys. Lett.* **2010**, 96.
(26) Kozlov, M. E.; Yakushi, K. *J. Phys.: Condens. Matter* **1995**, *7*, L209–L216.
(27) Watts, B.; Belcher, W. J.; Thomsen, L.; Ade, H.; Dastoor, P. C. *Macromolecules* **2009**, *42*, 8392–8397.
(28) Chen, D.; Nakahara, A.; Wei, D.; Nordlund, D.; Russell, T. P. *Nano Lett.* **2011**, *11*, 561–567.
(29) Collins, B. A.; Gann, E.; Guignard, L.; He, X.; McNeill, C. R.; Ade, H. *J. Phys. Chem. Lett.* **2010**, *1*, 3160–3166.
(30) Kiel, J. W.; Eberle, A. P. R.; Mackay, M. E. *Phys. Rev. Lett.* **2010**, *105*, 168701.
(31) Erb, T.; Zhokhavets, U.; Gobsch, G.; Raleva, S.; Stühn, B.; Schilinsky, P.; Waldauf, C.; Brabec, C. J. *Adv. Mater.* **2005**, *15*, 1193–1196.
(32) Vaynzof, Y.; Kabra, D.; Zhao, L.; Chua, L. L.; Steiner, U.; Friend, R. H. *ACS Nano* **2011**, *5*, 329–336.

■ NOTE ADDED AFTER ASAP PUBLICATION

This article posted ASAP on July 21, 2011. The Acknowledgment section has been revised. The correct version posted on July 29, 2011.